Journal of Cluster Science (2018) 29:599–603
https://doi.org/10.1007/s10876-018-1370-x

ORIGINAL PAPER

Magnetic Properties of the Triangular Lattice with Different Clusters: A Monte Carlo Study

A. Jabar[1] · R. Masrour[1]

Received: 7 July 2017 / Published online: 9 April 2018

Abstract
The magnetic properties of the triangular lattice with different clusters have been studied using the Monte Carlo simulations. The reduced transitions temperatures are deduced for different size of clusters L and for different exchange interactions. The variation of magnetization with the crystal field is given for different size of clusters and exchange interactions. Finally, the magnetic hysteresis cycles are found for different values of size of clusters and reduced temperatures. We found that the magnetic coercive fields increases with increasing the size of clusters and decreases with increasing the reduced temperatures.

Keywords Clusters · Transition temperatures · Exchange interactions · Magnetic hysteresis cycle · Magnetic coercive field

Introduction

In previous works [1, 2], the correlation identities and rigorous upper bounds on the critical temperature for the spin-1 Blume–Capel model on a Kagome lattice and spin correlation identities for the Blume–Emery–Griffiths model on Kagomé lattice are derived and combined with rigorous correlation inequalities lead to upper bounds on the critical temperature have been studied using the mean field approximation and the effective field approximation. The magnetic properties of ferrimagnetic mixed spins with integer and half integer and the spin-2 Blume–Emery–Griffiths model with four-spin interactions in a Blume–Capel model, using Monte Carlo simulations have been studied [3, 4]. The relation between a general spin-3/2 Ising model and an Ising model with two sets of Ising spins has been given in previous work [5]. The metallic nano-sized particles may show an ample variety of phenomena such as super-paramagnetism, magneto-resistance, magnetic anisotropy [6] which are relevant for innovative applications in very different fields ranging from medicine to microelectronics, magnetic storage devices and sensors. Previously, there are a number of studies on homogeneous Co clusters [7] and Pt clusters [8, 9]. Cluster Monte Carlo methods for the classical spin Hamiltonian of FePt with long range exchange interactions are presented [10] and the magnetic properties of $(ZnS)_n$ clusters (n = 1–16) due to 3D transition metals have been investigated using spin polarized density functional theory [11] and $(FePt)_n$ clusters (with nr5) have been studied within density functional theory [12]. Some clusters have potential application for many magnetic devices such as high-density recording media, magnetic bias films of magneto-resistive elements, and magnetic tips for magnetic force microscopy due to their high magnetic anisotropy and high coercive field [13, 14]. Experimentally, the comparative studies between such clusters and particles can elucidate surface structural characteristics of supported magnetic nanoparticles [15] and interface effect on the magnetic anisotropy of CoPt clusters has been also investigated [16]. The magnetic properties of Fe_n and Co_n clusters are mainly resulted from their valence electron configurations $3d^64s^2$ and $3d^74s^2$. Clusters consisting of more than one element have richer properties and are more interesting than clusters of pure elements [17]. Another characteristic of cluster that the magnetization measurement at room temperature indicates a weakly correlated cluster glass, as deduced from the approach to saturation that is well described with 2D

✉ R. Masrour
rachidmasrour@hotmail.com; r.masrour@uca.ma

[1] Laboratory of Materials, Processes, Environment and Quality, Cadi Ayyad University, National School of Applied Sciences, PB 63, 46000 Safi, Morocco

random anisotropy model [18]. The molecular dynamics simulations and graph-theory based cluster analysis have been used to compare self-assembly in systems of magnetic spheres, and cubes where the dipole moment is oriented along the side of the cube in the [001] crystallographic direction [19]. The renormalization group approach and scaling effect have been used to study the thermodynamic properties of the isotropic antiferromagnetic nearest-neighbour Ising model on the triangular lattice with three smallest clusters [20]. The paper is organized as follows: In the "Ising model" section we define the Ising model and in "Monte Carlo simulations" section the Monte Carlo simulations. Resulting magnetic properties of the triangular lattice with different clusters are presented and discussed in "Results and discussion" section. The final "Conclusions" section is devoted to conclusions.

Ising Model

We consider the triangular lattice with different clusters, as depicted in Fig. 1. Each site on the figure is occupied by an Ising spins S = 2. The Hamiltonian of this lattice includes nearest J, nearest neighbour J_3 neighbors interactions, and the crystal field Δ and external magnetic field h is given as:

$$H = -J \sum_{<i,j>} S_i S_j - J_3 \sum_{<i,j,k>} S_i S_j S_k - \Delta \sum_i S_i^2 - h \sum_i S_i \tag{1}$$

where $\langle i,j \rangle$ stand for the first nearest neighbor sites (i and j). $\langle i,j,k \rangle$ is over all triplets of sites belonging to elementary triangles. $<$ i, j, k $>$ is over all triplets of sites belonging to elementary triangles'', J_3 should be the nearest neighbour (NN) three-body spin–spin interaction. The spin moment is S = 2, we associate the 2S + 1 possible spin projections: ± 2, ± 1, 0. In full text the all physical ground are divided by J such as t = T/J, $R_3 = J_3/J$ and d = Δ/J.

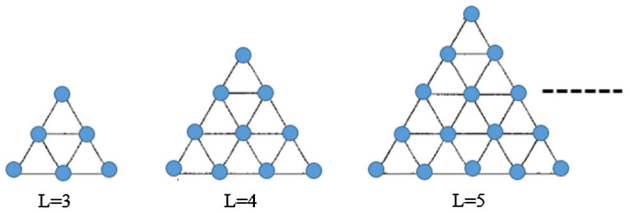

Fig. 1 The clusters for each case a L-cluster of size L with L(L + 1)/2 spins-2 where L = 3, 4, 5

Monte Carlo Simulations

The magnetic properties of the triangular lattice with different clusters with Ising ferrimagnetic is assumed to reside in the unit cells and the system consists of the total number of clusters N = L(L + 1)/2 where L = 3, 4, 5,…. We apply a standard sampling method to simulate the Hamiltonian given by Eq. (1). Cyclic free conditions on the lattice were imposed and were generated by sequentially traversing the lattice and making single-spin flip attempts. The flips are accepted or rejected according to a heat-bath algorithm under the Metropolis approximation. Our data were generated with 10^5 Monte Carlo steps per spin, discarding the first 10^4 Monte Carlo simulations. Starting from different initial conditions, we performed the average of each parameter and estimate the Monte Carlo simulations, averaging over many initial conditions. Our program calculates the following parameters, namely:

The internal energy per site E,

$$E = \frac{1}{N}\langle H \rangle \tag{2}$$

The magnetization of different size of clusters is given by:

$$M = \left\langle \frac{1}{N} \sum_i S_i \right\rangle \tag{3}$$

The magnetic susceptibility divided by the number of lattice site of different size of clusters is given by:

$$\chi = \beta \left(\langle M^2 \rangle - \langle M \rangle^2 \right) \tag{4}$$

where $\beta = \frac{1}{k_B T}$, T denotes the absolute temperature and k_B is the Boltzmann's constant.

Results and Discussion

The magnetic properties of the triangular lattice with different clusters have been studied using the Monte Carlo simulations.

We have presented in Fig. 2a, b, the magnetization and magnetic susceptibility, respectively divided by the number of lattice site of different clusters with $R_3 = 0$, d = 0 and h/J = 0.2. In Fig. 2b, the all magnetic susceptibilities are situated at the reduced transition temperature t_C. The obtained values of t_C for different size of clusters L = 3, 5, 7, 15 and 25 are 2.38, 4.8, 6.4, 7.8 and 9.6, respectively. The reduced transition temperature increases when the size of clusters increase. This behavior is comparable with that observed in previous work [20], but the obtained values are superior to those obtained by renormalization group approach and scaling effect for size L ≥ 3 in the same

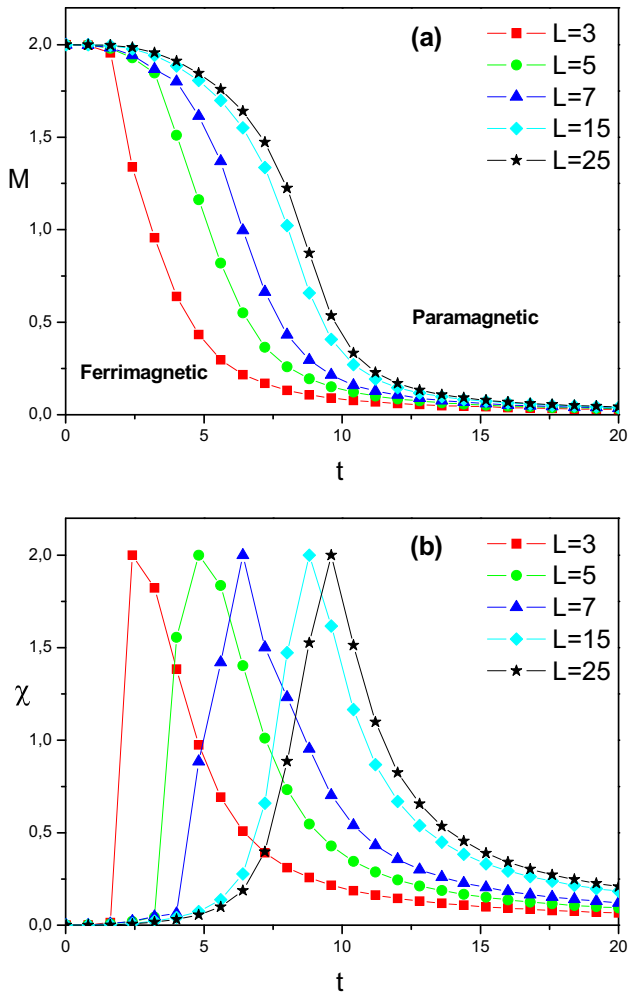

Fig. 2 The thermal total magnetization (**a**) and magnetic susceptibility (**b**) divided by the number of lattice site of different clusters with $R_3 = 0$, d = 0 and h/J = 0.2

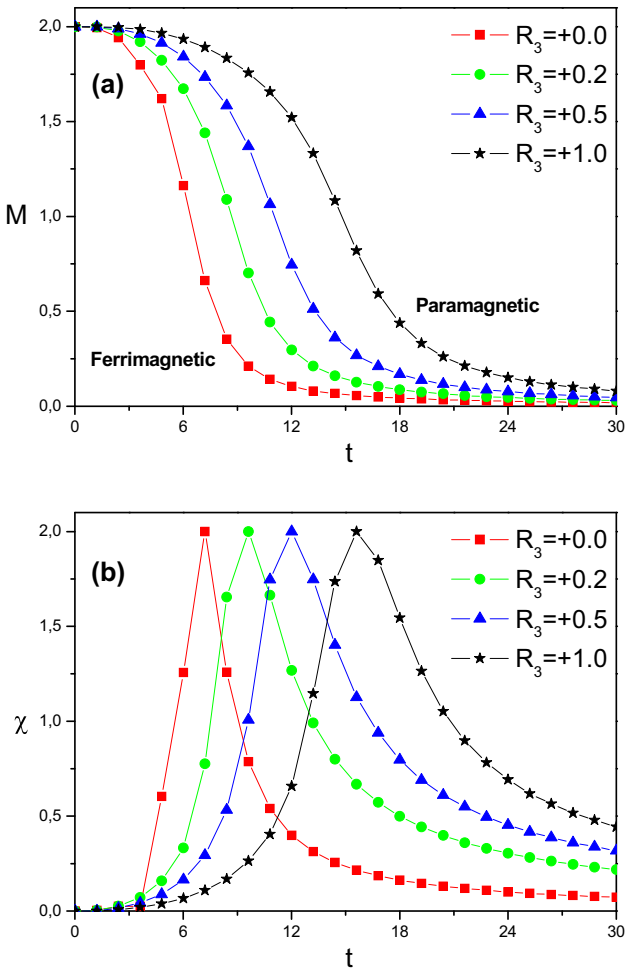

Fig. 3 The thermal magnetization (**a**) and magnetic susceptibility (**b**) divided by the number of lattice site of clusters with size L = 7 for $R_3 = +0.0, +0.2, +0.5, +1.0$ with d = 0 and h/J = 0.2

work. The ferrimagnetic to paramagnetic second order phase transition is observed for a higher values of clusters L = 5, 7, 15 and 25.

Fig 3a, b show, the magnetization and magnetic susceptibility, respectively divided by the number of lattice site of clusters with size L = 7 for $R_3 = +0.0, +0.2, +0.5, +1.0$ with d = 0 and h/J = 0.2. In Fig. 3, the all magnetic susceptibilities are also situated at the reduced transition temperature t_C. The obtained values of t_C for different size of clusters $R_3 = +0.0, +0.2, +0.5$ and +1.0 are 7.27, 9.6, 12 and 15.6, respectively for a fixed size L = 7. The reduced transition temperature increases with increasing the values of exchange interaction R_3. This behavior is comparable with that obtained on the magnetic properties in the one-dimensional Ising system study [21]. In Fig. 3a, the magnetic phase transition from paramagnetic to ferrimagnetic state is observed at the reduced transition temperature with L = 7 and for different values of R_3. We do not observe a bump in the curves of the magnetic susceptibilities for two curves (Fig. 3b). At $t = t_C$ the $\chi(t)$ curve has an anomaly whose form is typical of a second-order phase transition at t_C.

Figure 4a, b illustrate, the total and partial magnetization versus the crystal field d of different clusters L = 3, 5, 7, 15, 25, $R_3 = 0$ and different values of exchanges interactions $R_3 = +0.0, +0.1, +0.3, +0.5, +1.0$, L = 7, respectively for t = 1 and h/J = 0.2. The magnetization of different clusters increases with increasing the crystal field and exchange interaction until reached their saturation $M_S = 2$. For a high values of exchange interaction and size of cluster the magnetization increases quickly such as given in Fig. 4a, b.

Finally, we have given in Fig. 5a, b, the magnetic hysteresis cycles for different clusters L = 3, 5, 7, 25, t = 1 and different temperatures t = 1.0, 2.5, 4.5, 6.5 for a size of cluster L = 7, respectively with $R_3 = 0$ and d = 0. From Fig. 5a, we see that the magnetic coercive field increases

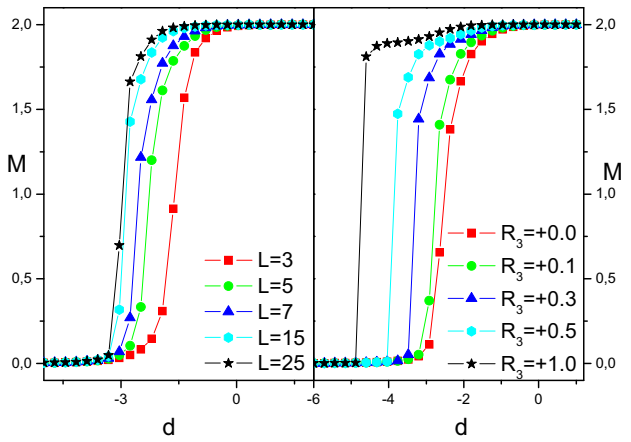

Fig. 4 The magnetization versus the crystal field d of different clusters L = 3, 5, 7, 15, 25, $R_3 = 0$ (**a**) and different values of exchanges interactions $R_3 = +0.0, +0.1, +0.3, +0.5, +1.0$, L = 7 (**b**) for t = 1 and h/J = 0.2

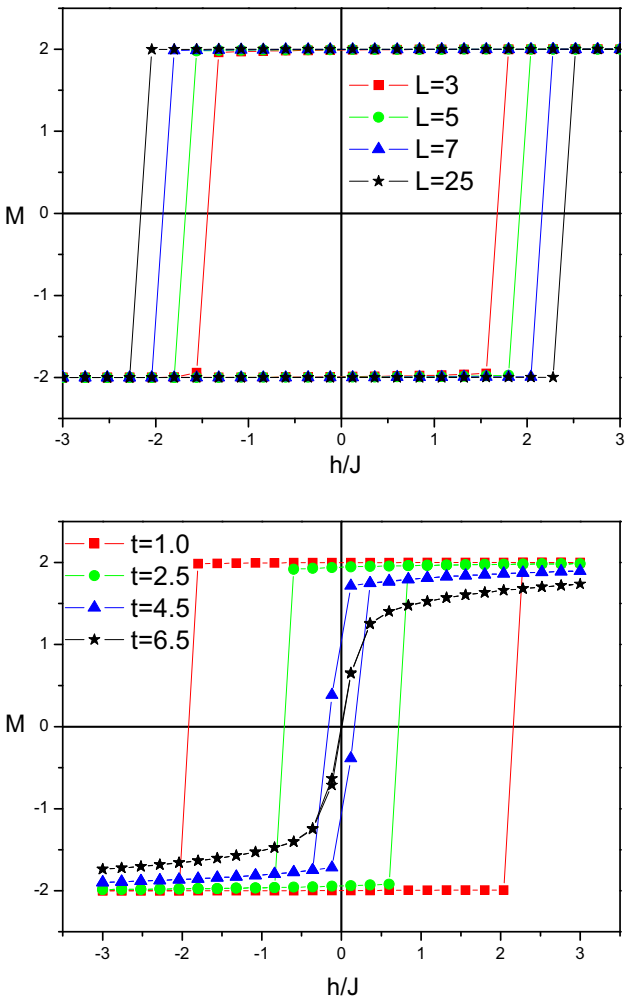

Fig. 5 The magnetic hysteresis cycles for different clusters L = 3, 5, 7, 25, t = 1 (**a**) and different temperatures t = 1.0, 2.5, 4.5, 6.5 for a size of cluster L = 7 (**b**) with $R_3 = 0$ and d = 0

with increasing the size of clusters. This result is comparable that given experimentally in previous work [22]. In Fig. 5b, we see that the magnetic coercive field decreases with increasing the reduced temperature values. The superparamagnetism behavior is observed at the reduced transition temperature because the magnetic coercive field is very weak. Same behavior is observed in previous work [23].

Conclusions

The magnetic properties of the triangular lattice with different clusters have been investigated using the Monte Carlo simulations. The reduced transitions temperatures are found for different size of clusters L and for different exchange interaction. The obtained values increase with increasing the size of clusters and exchange interaction. The magnetization increases with the crystal field, exchange interaction and size of clusters increasing. The magnetic hysteresis cycles are found for different values of size of clusters and for different reduced temperature value. The magnetic coercive fields increases with increasing the size of clusters and decreases when increases the reduced temperature. In the next work, we will study the kagome-lattice antiferromagnet using the numerical diagonalization of finite clusters and a finite-size scaling.

References

1. J. P. Santos and F. C. Sá Barreto (2015). *Physica A* **421**, 548–561.
2. J. P. Santos and F. C. Sá Barreto (2016). *Physica A* **442**, 22–35.
3. R. Masrour, A. Jabar, L. Bahmad, M. Hamedoun, and A. Benyoussef (2017). *J. Magn. Magn. Mater.* **421**, 76–81.
4. A. Jabar, R. Masrour, K. Jetto, L. Bahmad, A. Benyoussef, and M. Hamedoun (2016). *Superlat. Microstruct.* **100**, 818–825.
5. T. Horiguchi and Y. Honda (1995). *Prog. Theor. Phys.* **93**, (5), 981–985.
6. J. Bansmann, S. H. Baker, C. Binns, J. A. Blackman, J. P. Bucher, J. Dorantes-Dávila, V. Dupuis, L. Favre, D. Kechrakos, A. Kleibert, K. H. Meiwes-Broer, G. M. Pastor, A. Perez, O. Toulemonde, K. N. Trohidou, J. Tuaillon, and Y. Xie (2005). *Surf. Sci. Rep.* **56**, 189–275.
7. M. Pereiro, S. Man'kovsky, D. Baldomir, M. Iglesias, P. Mlynarski, M. Valladares, D. Suarez, M. Castro, and J. E. Arias (2001). *Comput. Mater. Sci.* **22**, 118.
8. A. Sebetci and Z. B. Guvenc (2003). *Surf. Sci.* **525**, 66–84.
9. L. Xiao and L. Wang (2004). *J. Phys. Chem. A* **108**, 8605.
10. A. Lyberatos and G. J. Parker (2016). *J. Magn. Magn. Mater.* **400**, 266–270.
11. N. Kaur, K. L. Singh, and H. Sharma (2015). *J. Magn. Magn. Mater.* **388**, 160–166.
12. K. Boufala, L. Fernandez-Seivane, J. Ferrer, and M. Samah (2010). *J. Magn. Magn. Mater.* **322**, 3428–3437.
13. S. H. Liou, S. Huang, E. Kimek, R. D. Kirby, and Y. D. Yao (1999). *J. Appl. Phys.* **85**, 4334.

14. N. Li and B. M. Lairson (1999). *IEEE Trans. Magn.* **35**, 1077.
15. G. C. Papaefthymiou (2004). *J. Magn. Magn. Mater.* **272–276**, e1227–e1229.
16. S. Rohart, C. Raufast, L. Favre, E. Bernstein, E. Bonet, W. Wernsdorfer, and V. Dupuis (2007). *J. Magn. Magn. Mater.* **316**, e355–e359.
17. Y. Zhang, Y.-N. Duan, J.-M. Zhang, and X. Ke-Wei (2011). *J. Magn. Magn. Mater.* **323**, 842–848.
18. R. Morel, A. Brenac, C. Portemont, T. Deutsch, and L. Notin (2007). *J. Magn. Magn. Mater.* **308**, 296–304.
19. E. S. Pyanzina, A. V. Gudkova, J. G. Donaldson, and S. S. Kantorovich (2017). *J. Magn. Magn. Mater.* **431**, 201–204.
20. A. H. Lacerda, A. J. F. De Souza, and F. G. B. Moreira (1989). *Physica A* **155**, 337–351.
21. N. Şarlı (2014). *Physica E* **63**, 324–328.
22. X. W. Wu, et al. (2006). *J. Magn. Magn. Mater.* **303**, e261–e264.
23. E. Kantar and M. Ertaş (2014). *Solid State Commun.* **188**, 71–76.